



OPEN RACK1 contributes to the upregulation of embryonic genes in a model of cardiac hypertrophy

Marcello Ceci¹, Davide Bonvissuto², Flavia Papetti¹, Federica Silvestri¹, Claudio Sette^{2,3}, Elisabetta Catalani⁴, Davide Cervia⁴, Rosalba Gornati⁵ & Nicla Romano¹✉

Receptors for activated C kinases (RACKs) have been shown to coordinate PKC-mediated hypertrophic signalling in mice. However, little information is available on its participation in embryonic gene expression. This study investigated the involvement of RACK1 in the expression of embryonic genes in a zebrafish (ZF) ex vivo heart culture model by using phenylephrine (PE) or a growth factors cocktail (GFs) as a prohypertrophic/regeneration stimulus. Blebbistatin (BL) inhibition has also been studied for its ability to block the signal transduction actions of some PEs. qRT-PCR and immunoblot analyses confirmed the upregulation of RACK1 in the PE- and GFs-treated groups. BL administration counteracted PE-induced hypertrophy and downregulated RACK1 expression. Immunohistochemical analyses of the heart revealed the colocalization of RACK1 and embryonic genes, namely, *Gata4*, *Wt1*, and *Nfat2*, under stimulation, whereas these genes were expressed at lower levels in the BL treatment group. Culturing ZF heart cells activated via GFs treatment increased the expression of RACK1. The overexpression of RACK1 induced by the transfection of recombinant RACK1 cDNA in ZF heart cells increased the expression of embryonic genes, especially after one week of GFs treatment. In summary, these results support the involvement of RACK1 in the induction of embryonic genes during cardiac hypertrophy/GFs stimulation in a fish heart model, which can be used as an alternative study model for mammals.

Keywords Cardiac hypertrophy, RACK1, Zebrafish, GATA4, WT1, NFAT2, Heart, Phenylephrine, Growth factors, Blebbistatin

Receptor for activated C kinase 1 (RACK1) is a member of the tryptophan-aspartate repeat (WD-repeat) family of proteins with homology to the β subunit of G proteins^{1,2}. Although WD-repeat proteins lack enzymatic activity, they are subject to posttranslational modifications, suggesting that their cellular location and function can be reversibly modulated³. RACK1, constituted by WD folders, appears to play multiple roles in the cell and serves as a hub for diverse signal transduction pathways⁴. The association of RACK1 with the active conformation of PKC favours eIF6 phosphorylation and acts as a component of alternative eIF3d-dependent translation⁵⁻⁷. Additionally, RACK1 represses translation by binding to the ArgonAUTA/miRNA (miRISC) complex in both invertebrates and vertebrates⁸. Altering RACK1 expression impacts miRISC functions and impairs the association of the complex with the translating ribosomes⁹. RACK1 also plays an important role in the nucleus by activating P300 protein-dependent acetylation of nucleosomes¹⁰. Owing to its multiple functions, RACK1 expression is essential, and RACK1 knockout mice die during embryonal development¹¹. In the mouse heart, PKC-RACK interactions and RACK expression modulate PKC-mediated manifestation of the cardiac phenotype; in particular, cardiac-specific transgenic overexpression of PKB subunit (PKC β II) cDNA provoked cardiac hypertrophy¹².

RACK1 signal transduction cascades, which are associated with cardiac hypertrophy, have yet to be elucidated¹⁰. RACK1 may be involved in the activation of mammalian cardiac fibroblasts and their transformation into active myofibroblasts, which are responsible for excessive extracellular matrix production and deposition, which is typical of cardiac fibrosis^{13,14}. This process is due to RACK1 activity and the downregulation of key miRNAs, such as miR133a and miR1¹⁵. Recently, research in mice established a correlation between the Speckle-type pox virus-zinc finger (POZ) protein and RACK1 in heart fibrosis¹⁶.

¹DEB, University of Tuscia, Viterbo, Italy. ²DNHA, Catholic University of Sacred Heart, Rome, Italy. ³IRCCS, Policlinico A. Gemelli Foundation, Rome, Italy. ⁴DIBAF, University of Tuscia, Viterbo, Italy. ⁵DBSV, Insubria University, Varese, Italy. ✉email: nromano@unitus.it

Some differences in fibroblast activation between zebrafish (ZF) and mammals have been reported. In ZF, cardiac hypertrophy is characterized by hyperplasia and a growing number of myofibrils in myocytes¹⁷. Resident ZF fibroblasts deposit fewer connective fibrils than do mammalian fibroblasts and are eventually pushed to transdifferentiate into myocytes and components of the vascular system^{18,19}. This process occurs in both regeneration and hypertrophy-induced processes through the downregulation of miR1, miR133a, and miR133b, which directly or indirectly control the expression of embryonic genes such as Gata binding protein 4 (GATA4), nuclear factor of activated T cells-2 (NFAT2), and Wilms tumor-suppressor gene-1 (WT1)^{17,18}. In the hypertrophy process induced by phenylephrine (PE), cells undergo tonic contraction through the involvement of various calcium channels in the inner and plasma membranes. The resulting calcium waves can activate PKC phosphorylation processes, miR-downregulation, RACK1 activation and re-expression of embryonic genes^{10,17,20}.

We previously demonstrated that microRNAs (miR1, miR133a, and miR133b) are essential for controlling the expression of key embryonic genes involved in differentiating cardiac tissue components (epicardium, myocardium, and endocardium) during ZF heart regeneration and in PE-induced hypertrophy^{17,18,21,22}. Moreover, blebbistatin (BL) was shown to counteract the activity of PE, probably by blocking calcium waves²². In this study, by using the same ex vivo culture model of the ZF heart, we aimed to determine the role of RACK1 in embryonic gene re-expression during the cardiac hypertrophy process.

Materials and methods

The study was conducted in accordance with the guidelines from Directive 2010/63/EU of the European Parliament on the protection of animals used for scientific purposes and was approved by the protocol code N. 10-87/2010 (and the upgrades until 2020) authorization/s from the Italian Health Ministry. All methods have been done and reported in following with ARRIVE guidelines.

Ex-vivo experiments

Adult of ZF ($n = 339$ of which 162 female and 177 male), strain Tuebingen (WT, PETRA-AQUA s.r.o., Czech Republic) weighing 0.40 ± 0.05 g and lengths of 3.4 ± 0.07 cm were used for the experiments. No particular criteria were set for including and excluding animals. The ZF were gently placed in a tray containing the dose 4 mg/ml ethyl 3-aminobenzoate methanesulfonate salt (MS222, cat. A5040, Sig-ma-Aldrich/Merck/Merck) necessary to put fish to death (MS222 used both to do firstly anesthesia and, after 10 min, also euthanasia, according to the ARRIVE essential 10 guidelines). In a flow laminar hood (PBI, International), the fish was placed on a sponge and under microscope to remove the heart. The heart was extracted and washed in L15c media [L15, Liebovitz buffer cat. L5520, Sigma-Aldrich/Merck] supplemented with 80 units penicillin/streptomycin (Sigma-Aldrich/Merck) + 0.5 mg/ml L-glutamine (Sigma-Aldrich/Merck) + 5% fetal calf serum (GIBCO) and 0.8 mM CaCl₂ (Sigma-Aldrich/Merck) and transferred to 12-well Petri dishes and divided into four groups: (1) the control (CTR) cultured with L15c medium; (2) the batch treated with phenylephrine 500 μ M (PE, L-phenylephrine, cat. P1240000, Merck) for 96 h; (3) the batch treated with a cocktail of growth factors (GFs); and (4) the batch treated simultaneously with PE and blebbistatin (BL, (-) blebbistatin, cat. B0560, Sigma-Aldrich/Merck) 10 μ M for 96 h (PE/BL). This latter group was considered to confirm the inhibitory action of BL on treatment with PE. To evaluate the inhibitory effects of BL on PE, the other two experimental groups were used: (5) the batch treated with PE for 72 h and then treated with BL for 24 h (called PE + BL), and (6) the batch treated with BL for 24 h and then treated with PE for 72 h (called BL + PE). The cocktail of GFs was developed in our laboratory and has already been published²¹. Briefly, L15c was spiked with a mixture enriched with growth factors consisting of 5 ng/ml recombinant human Cardiotropin-1 (CT, Peprotech, Inc.), 2 nM thrombin (TR, Sigma-Aldrich), 40 ng/ml recombinant human, fibroblast growth factor-basic (FGFb, FGF2, Invitrogen, Biosource), 10 ng/ml fibroblast growth factor-4 (FGF-4, Sigma-Aldrich/Merck) and 10 ng/ml platelet-derived growth factor-BB (PDGF-BB, Sigma-Aldrich/Merck).

RNA extraction and qRT-PCR analysis

The collected hearts ($n = 6$ in triplicate experiments) were placed in 0.5 mL of RNeasy lysis solution (stabilization solution, Invitrogen, US) and stored at -80 °C. The extraction and purification of total RNA were performed via a previously published procedure²². Briefly, after the isolation and purification of total RNA via Thermo Fisher Kits (US), the quantity and purity of the extracted RNA (A260/280 ratio) were tested via the Molecular Device SpectraMax QuickDrop SPM. An Agilent Bioanalyzer 2100 with an RNA 6000 Pico Kit was used to verify the integrity of the RNA. The TaqMan GEX Assay (Thermo Fisher/Applied Biosystem) was used in combination with DNase directly in the sample already extracted. For these cDNAs, amplification via real-time PCR was performed via PowerUp SYBR Green Master Mix and appropriate primers: Receptor for Activated C Kinase 1 (RACK1, Dr03118827_m1), Myosin Heavy Chain 7 (MYH7, Dr-03431146_m1), Brain Natriuretic Peptide (BNP, specific for ZF ventriculus, ID ARAADCC) and S18 (HS99999901_S1) were purchased as primers from Thermo Fisher Scientific (US). The relative expression of the genes was calculated by comparing the cycle times for each target PCR. The Ct values of each PCR target were normalized by subtracting the cycle threshold (Ct) value of S18, which was represented by the value Δ Ct. The level of relative expression was calculated via the following equation:

$$\text{Relative gene expression} = 2^{-(\Delta\text{Ct}_{\text{sample}} - \Delta\text{Ct}_{\text{control}})}$$

Significant differences (probability values, p) between the experimental groups and control/untreated animals were calculated on the basis of the means from three parallel experiments \pm standard deviations (SDs) and analysed via one-tailed ANOVA-Bonferroni correction. One-way ANOVA is used to evaluate the difference

in means between three or more groups, taking into account only the groups and no other factors. Bonferroni correction is applied in comparisons among groups that are not too large and permits the collection of correct statistical data.

Immunoblot analysis

The hearts ($n=10$ for each group in triplicate experiments) were homogenized manually with a pestle in lysis buffer [Tris-HCl (20 mM, pH 7.4) + EGTA (10 mM) + NaCl (150 mM) + Triton X-100 (1%, Sigma-Aldrich/Merck) glycerol (10%, Sigma-Aldrich/Merck) + sodium dodecyl sulfate (SDS, 1%, Sigma-Aldrich/Merck)] supplemented with protease and phosphatase inhibitors (PPIs). Protein extraction from cells was performed in RIPA buffer [Tris-HCl (10 mM, pH 8.0) + NaCl (140 mM), EDTA (1 mM, Sigma-Aldrich/Merck) + Triton X-100 (1%, Sigma-Aldrich/Merck) + SDS (0.1%)] supplemented with PPIs. Following the standard protocol, the proteins were quantified with a BCA protein assay kit (Pierce, Rockford, IL, USA). Proteins were loaded on 4–20% polyacrylamide precast gels from 30 to 50 μg of total protein (TGX Stain-free precast gels; Bio-Rad). The blotted proteins were transferred onto a nitrocellulose membrane via a Trans-Blot Turbo SystemTM (7 min at 2.5 A) and a Transfer PackTM (Bio-Rad). The primary antibodies used were anti-mouse RACK1 IgM (Bioscience, US) and rabbit anti-actin (Invitrogen, US). After incubation with the appropriate horseradish peroxidase-conjugated secondary antibody, the bands were visualized via the Clarity Western ECL substrate with a ChemiDoc MP imaging system (Bio-Rad). Bands were quantified for densitometry using Bio-Rad Image Lab software.

Histology and immunohistochemistry

Sample preparation for histology and immunohistochemistry

The hearts cultured *ex vivo* ($n=7$ for each group) were placed in a fixed solution of 4% paraformaldehyde in PBS (Santa Cruz Biotechnology, US) + 10% sucrose for 24 h at 4 °C. The fixed hearts were incubated overnight in PBS containing 10% sucrose. Some heart samples (three from each group) were embedded in paraffin. The sections obtained with a Reichert-OME microtome were mounted on APES-treated slides (Sigma-Aldrich). The dewaxed sections were processed for histochemistry and DAB immunohistochemistry. The other hearts (4 from each group) were embedded in OCT compound (Invitrogen) at -40 °C and sectioned with a cryomicrotome (Leitz) for fluorescence-immunohistochemistry. Superfrost Plus Gold (Espredia, NL/USA) slides were used. The sections were observed with an AxioScope (Zeiss) microscope supported with software for image analysis (Axiovision 100 software, Zeiss). The confocal images were acquired by a Zeiss LSM 710 scanning module with 34 spectral R/FL detection channels and 6 laser lines (405, 458, 488, 514, and 633 nm) by acquiring at least 6–8 analysis plans.

Masson's trichrome staining

The deparaffinized sections were stained following the procedure published in²² and described in the supplementary material.

Immunohistochemistry

The cryosections obtained from 4 hearts of each group ($N=24$) were treated with phosphate buffer (PBS) supplemented with 2% Tween + 1 mM EDTA (Sigma-Aldrich/Merck), and the slides were placed in citrate buffer to visualize the antigens for 20 min at 40 °C. Subsequently, the slides were washed with PBSTX (0.8% Triton X-100 in PBS). The sections were treated for 12 h with 0.01% Sudan Black (Sigma-Aldrich/Merck) in PBSTX. The sections were then processed in 0.1% Triton X-100 (Sigma-Aldrich/Merck) + 0.1% DMSO (Sigma-Aldrich/Merck) + 2% BSA (Sigma-Aldrich/Merck) and incubated at 4 °C with the primary antibodies. The primary antibodies used were as follows: (1) anti-Wilms Tumour 1 (WT1, rabbit recombinant polyclonal protein antibody, Abcam) 1:100¹⁷ or (2) anti-Gata4 (GATA4 rabbit recombinant polyclonal protein antibody, Abcam) 1:100²¹ or (3) anti-Nfat2 (NFAT2 rabbit recombinant polyclonal protein antibody, Abcam) 1:1500¹⁷. These antibodies were used in conjunction with the RACK1 anti-mouse IgM antibody (BD, Bioscience, USA). The antibodies were diluted in PBST + 1% normal goat serum (NGS, Sigma-Aldrich/Merck). After 48 h of incubation at 4 °C, the slides were washed with PBSTX and incubated with PBSTX + 1% NGS (Sigma-Aldrich/Merck) + 2% BSA before they were incubated with the following fluorophore-conjugated secondary antibodies: (1) red fluorescent goat anti-mouse IgM (GAM, 1:200, Alexa-conjugates 594 wavelength, Invitrogen) and (2) green fluorescent goat anti-rabbit (GAR, 1:200, Invitrogen, 488 nm wavelength) for 1 h at room temperature. The nuclei were counterstained with 4',6-diamidin-2-fenilindolo (DAPI, 1:1000, Vectastain). Slides were mounted with Fluoreshield Mounting medium. The confocal analysis was performed by using a ZEISS LSM 710-scanning module with 34 spectral R/FL detection channels and 6 laser lines (405, 458, 488, 514, and 633 nm) with at least six analysis plans for each sample. To obtain a correct and standardized fluorescence intensity from the samples, each fluorescence channel was first set on a sample treated only with secondary antibodies/DAPI and then set on the control sample without treatments (CTR group). The analysis of antibody staining was as follows: WT1/RACK1/DAPI; NFAT2/RACK1/DAPI; and GATA4/RACK1/DAPI immunostaining was carried out on a single section. Each image acquired from the relative fluorescent canal was converted to RGB, merged for the three color canals, and normalized to the background by the Adobe Photoshop 6 program (Adobe Systems, Mountain View, CA, USA). The resolution of each image was selected to be 1024 × 1024 pixels (single stack).

Cell culture, RACK1/HA transfection and immunocytochemistry

Cell culture

Nine hearts were cultured in growth factor (GF) medium composed of basic cardiac medium (L15-Sigma/Aldrich) supplemented with 100X penicillin/streptomycin, 0.5 mg/ml L-glutamine, 5% fetal calf serum (FCS, GIBCO), 0.8 mM CaCl₂ spiked with a mixture enriched with growth factors consisting of 5 ng/ml recombinant

human Cardiothrophin-1 (CT, Peprtech Inc.), 2 nM thrombin (TR, Sigma-Aldrich/Merck), 40 ng/ml recombinant human, fibroblast growth factor-basic (FGFb, FGF2, Invitrogen, Biosource), 10 ng/ml fibroblast growth factor-4 (FGF-4, Sigma-Aldrich) and 10 ng/ml platelet-derived growth factor-BB (PDGF-BB, Sigma-Aldrich/Merck) and maintained for 24 h post explantation as described previously²¹. After that period, the nonadherent cells were collected and used to prepare primary cultures of cardiac-activated cells. The cells were distributed in triplicate in wells of polystyrene plates with 0.5 ml each of GF medium. Some of the cells were used for immunocytochemistry with double staining for RACK1/WT1, RACK1/NFAT2, and RACK1/GATA4. The nuclei were stained with DAPI (1:1000, Vectastain). The other part was used to transfect the cells or, as a control, was maintained with lipofectamine/medium (see Sect. 2.5.3).

Immunocytochemistry of cytosin cells (CSc)

Approximately 100 μ l of cultured cells were taken from the wells, fixed with 4% PFA in PBS + 20% sucrose, centrifuged at 1000 rpm for 10 min at 9°C on slides (Superfrost Plus Gold-Espredia, NL/USA), and dried for 15 min at room temperature under UV-steril flow. Once dry, the pellets on the CSc-slide were washed with 500 μ l of PBS for 5 min and processed for immunostaining. The CSs were washed with PBSTX 0.8% 15' followed by unmaskin solution (20'/37°C) and subsequently washed with PBSTX 0.8% 10'/RT. The slides were incubated in Sudan black solution (0.01 g/70% alcohol, Sigma-Aldrich), treated with 5% H₂O₂ in PBSTX for 10 min to eliminate possible autofluorescence due to peroxisomes, and then washed with 0.8% PBSTX. The slides were treated with nonspecific blocking reagent (normal mouse serum 1% (Sigma-Aldrich/Merck), normal goat serum 1%, and bovine serum albumin 2% in PBSTX). The slides were finally incubated with a mixture of primary antibodies against RACK1/WT1, RACK1/GATA4, or RACK1/NFAT2 for 12 h at 4°C. As a control for the reaction, a slide was treated with the solution used to dilute the antibodies (PBSTX 0.8 + BSA 1%). After 12 h, the slides were washed in PBSTX 0.8% and treated with PBSTX 0.8% + BSA 5% to block the nonspecific reaction of secondary antibodies. The slides were treated with a mixture of secondary antibodies: goat-anti-rabbit-green fluorescent (GAR-FITC, Alexa Fluor 488 nm, 1:200, Invitrogen)/goat-anti-mouse-red fluorescent (GAM-TRITC, AlexaFluor 586 nm, Invitrogen) in PBS supplemented with 5% BSA (Sigma-Aldrich) and mounted with 25 μ l of PBS-glycerol/DAPI (Sigma-Aldrich). The slides were observed with an AxioScope microscope (Zeiss) equipped with image analysis software.

Transfection procedure

The protocol has been adapted to ZF cells from²³. One day before transfection, 0.5×10^5 cells were seeded per well in 500 μ l of 1:1 Opti-MEM I (Invitrogen/31985)/basic medium (without antibiotics/fetal calf serum until the time of transfection, L15-OT). For each transfection sample, DNA-Lipofectamine 2000 complexes were prepared by diluting 0.8 μ g of DNA (containing *Rack1* and *hemagglutinin*; RACK1/HA Invitrogen, V79020) in 50 μ l of Opti-MEM I. In parallel, a control of Transfection (CTR) was prepared using 50 μ l of Opti-MEM without RACK1/HA. Four microliters of Lipofectamine 2000 (Thermo Fisher Scientific US/IT) was diluted in 100 μ l of Opti-MEM I, and after mixing gently, the mixture was divided into two Eppendorf vials. After 5 min at room temperature, the liquid Lipofectamine/Opti-MEM I from each vial was added to the Eppendorf without plasmid (CTR) or to the Eppendorf with the plasmid (RACK1/HA) to reach a final volume of 100 μ l each. Two vials containing 100 μ l of the transfection mixture were added to each well containing cells and L15-OT. The buffers/cells in the wells were mixed gently by rocking the plate back and forth under sterile flow. The plate was incubated at 28°C in a humidified incubator for 24 h until transgene expression (T0 and T1) was assayed. Owing to the low metabolism of healthy cells, incubation for 24 h was necessary to achieve 80% transfection success. After this period, the cells were washed in osmolar PBS and centrifuged at 1000 rpm/10'. Half of the cells were fixed with a mixture of PFA 4%/PBS added to 5% sucrose at 4°C for 24 h (called the T0 samples). The remaining part was added to CTR or RACK1/HA wells containing L15c/GFs supplemented with 1% gentamicin (to prevent the expulsion of RACK1/HA plasmids), and the plate was placed in a cell incubator at 28°C. L15c/GFs (150 μ l) were added to the wells two times per week (samples were referred to as T1). After this period, the transfected and control cells were washed with osmolar PBS, centrifuged at 1000 rpm/10', and fixed as described above.

An immunocytochemical assay was performed on CSc (CTR and RACK1/HA from the T0 and T1 samples) on poly-L-lysine-coated slides (Bright-GB). Double immunostaining was performed as described in Sect. 2.5.2. The primary antibodies used were as follows: (1) rabbit anti-hemagglutinin (batch C29F4/Thermo Fisher Scientific (US), 1:100; HA-TAG) in combination with (2) mouse anti-RACK1 (see above) to ascertain the presence of both in the cells. To study the presence of RACK1+ in the transfected cells in combination with the eventually increased expression of embryonic genes, (3) a mouse HA-TAG monoclonal antibody (Ab1424, Abcam (UK) 1:200) in combination with (4) rabbit-NFAT2, rabbit-WT1 or rabbit-GATA4 (see above) was used.

The secondary antibodies (IIAbs) used were green-fluorescent Alexa Fluor® 488-conjugated goat anti-mouse IgG (1:200, Invitrogen, US) and Alexa Fluor® 596-conjugated goat anti-rabbit IgG (1:200, Invitrogen, US). The IIABs were incubated at room temperature for 30 min, washed in 0.8% PBST, and then coated with PBS/glycerol/DAPI mounting media (Sigma-Aldrich, US) and cover glass. As controls for the immunohistochemical reactions, cytoslides marked with secondary antibodies (i.e., GAM and GAR) in combination with DAPI were used to avoid false positives. The confocal analysis of immuno-marked slides was performed via a ZEISS LSM 710 instrument with a combination of four to six plans for laser scanning. To obtain a correct and standardized fluorescence intensity from the samples, each fluorescence channel was first set on a sample treated only with secondary antibodies/DAPI and then set on the control sample without treatments (CTR group).

Results

RACK1 is co-expressed with hypertrophy markers in the ZF heart

Morphological analysis of cardiac tissue treated with GFs or PE via Masson trichomic staining confirmed the hypertrophy induced by PE and the counteracting effects of BL²². GFs treatment caused a slight increase in the number of myofibrils in the explanted ZF heart, accompanied by moderate hyperplasia of epicardial cells (Supplementary Materials, Fig. S1). Thus, similar to PE treatment, GFs treatment did not affect hypertrophy; rather, it was only a proliferation stimulus. To test whether hypertrophy and/or hyperplasia affect the expression of RACK1, cardiac myosin/heavy chain 7 (MYH7) and brain natriuretic peptide (BNP), a hypertrophy marker specific to the ventricular portion of the heart, we performed quantitative real-time PCR (qRT-PCR) analyses of RNA isolated from ZF hearts subjected or not subjected to ex vivo treatments. These analyses (Fig. 1) revealed that PE and GFs treatment increased the expression of RACK1 (PE and GFs vs. CTR or other groups (*); ANOVA-Bonferroni correction $p < 0.001$). The samples treated simultaneously with PE and BL (PE/BL) or PE + BL showed no significant changes. In contrast, compared with those in the control group, the RACK1 expression in the PE-treated group was significantly lower (BL + PE vs. CTR, $p < 0.05$, **). MYH7 expression (Fig. 1) was significantly upregulated in PE but also in PE + BL and GFs (*). The highest expression was observed in the PE treatment group, with statistical significance in all the other groups ($p < 0.001$ or $p < 0.005$, ANOVA-Bonferroni correction), indicating increased expression of this sarcomeric myosin in the PE-treated hearts. The PE + BL group presented an increase in MYH7 (vs. CTR, $p < 0.01$). Compared with the CTR group, the GFs group presented a slight increase (GFs vs. CTR, $p < 0.05$). BNP was increased in the PE group (PE vs. CTR; $p < 0.001$, *), PE group vs. all other groups $p < 0.001$ (**, ANOVA-Bonferroni correction) and PE + BL group (PE + BL vs. CTR $p < 0.01$). Conversely, this upregulation was partially repressed after pre- and cotreatment with BL. The GFs also presented a greater mean than did the control, but the variability among the samples was not statistically significant.

Immunoblot analysis of RACK1 expression

Western blot analyses (Fig. 2) were performed to evaluate the Rack1 protein (RACK1) expression level in treated heart samples (PE, PE/BL, PE + BL, BL + PE, and GFs). The normalization of actin levels indicated that, compared with the CTR group, the PE-treated group presented a fourfold increase in RACK1 expression (Fig. 2, $p < 0.001$, *). The other treatment groups also presented slight increases in the presence of protein. In particular, the GFs increased ($p < 0.05$, *). The PE + BL group expressed less protein than the CTR group did (**; $p < 0.05$), in contrast with the mRNA quantified via qRT-PCR.

Localization of RACK1 in tissue

Immunohistochemistry analysis via nickel enhancement/DAB on whole hearts revealed RACK1 positivity at the level of the epicardium, endocardium, and myocardium (Fig. S2, supplementary data). In particular, compared with untreated control hearts, hearts treated with PE or GFs showed detectable staining for RACK1 at the epicardium and endocardium levels (CTR vs. PE vs. GFs Figure S2, Supplementary Data). Hearts treated simultaneously with PE and BL were positive in the epicardium, which was greater than that of the untreated control but less intense than that of the PE and GFs. In contrast, hearts pretreated with PE showed an intense reaction at the level of muscle fibres and the epicardium compared with those in the untreated control hearts but were less intense than those in the PE- and GF-treated hearts. In particular, the endocardium was markedly lower in the PE-treated group than in the GFs-treated group. The patterns of the hearts posttreatment with PE were similar to those of the GFs.

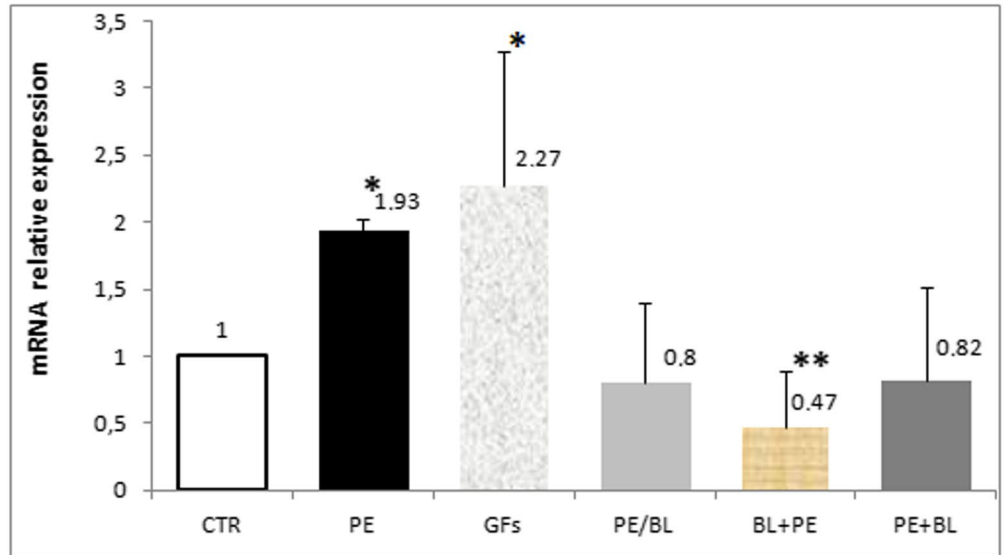
Immunohistochemistry and cytochemistry of RACK1/embryonal markers support their colocalization in tissue

To verify whether RACK1 colocalized with embryonic gene expression, a double-labelling confocal analysis was conducted with different RACK1 embryonic markers (Figs. 3, 4 and 5, merged staining data: S3—Supplementary Data; GATA4, WT1, NFAT2;). All the sections showed RACK1 labelling similar to that observed with DAB/nickel-enhanced immunohistochemistry while highlighting its coexpression with different embryonic genes (GATA4, WT1, and NFAT2 proteins). In particular, GATA4 (Fig. 3) is expressed in the epicardium, endocardium, and myocardium, resulting in complete overlap with RACK1 expression. The colocalization of WT1 with RACK1 (Fig. 4) resulted in exclusive positivity in the epicardium. The NFAT2 (Fig. 5) marker was clearly positive in the endocardium lining cardiomyocytes and colocalized with RACK1. In heart samples from plants treated with GFs, the staining of these proteins was similar to that in the PE group, but the expression of embryonic markers was lower. In the PE/BL group (treated simultaneously with PE and BL), RACK1 positivity was greater than that in the control. This positivity was mainly localized around the fibres (in cardiomyocytes), where it colocalized with GATA4 and NFAT2. Furthermore, WT1 positivity in the epicardium was less marked. In contrast, in hearts pretreated with PE, GATA4 staining was intense and greater than RACK1 positivity. WT1 and NFAT2 showed less intense reactions in the epicardium and endocardium, respectively, than did PE and GFs. Post-PE-treated hearts presented a less intense reaction to RACK1 and a lower signal for cardiac markers. The merged images of RACK1/GATA4/DAPI, RACK1/WT1/DAPI, and RACK1/NFAT2/DAPI staining are shown in the Supplementary Materials (Figure S3).

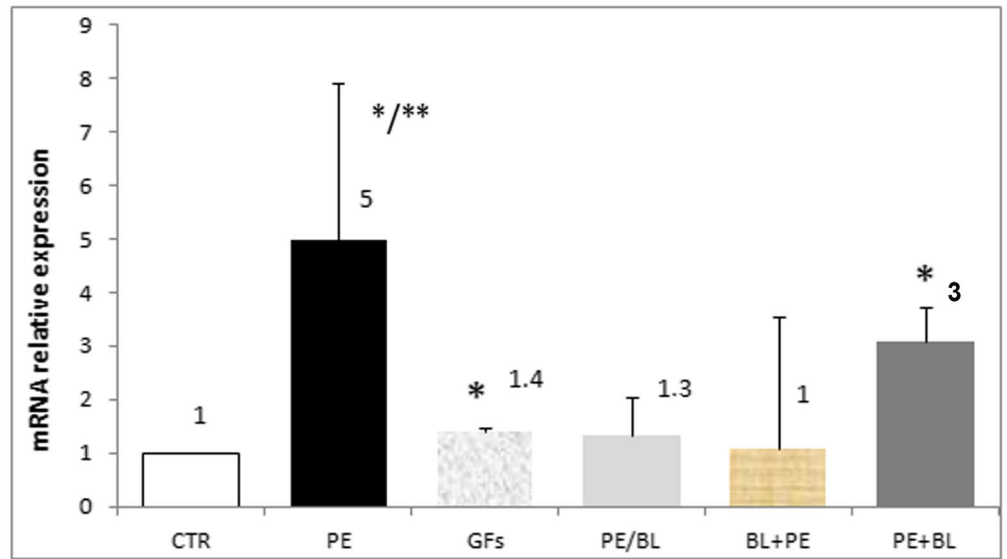
Rack1+ transfected epicardial/endocardial cells presented increased expression of embryonal markers

Cardiac cells activated by GFs in ex vivo cultured hearts leave the organ as transdifferentiated cells and start to proliferate in the culture buffer. Previously, we identified two types: epicardium-activated and endocardium-activated cells that express embryonal genes. In particular, activated Epicardium expresses WT1/GATA4, and

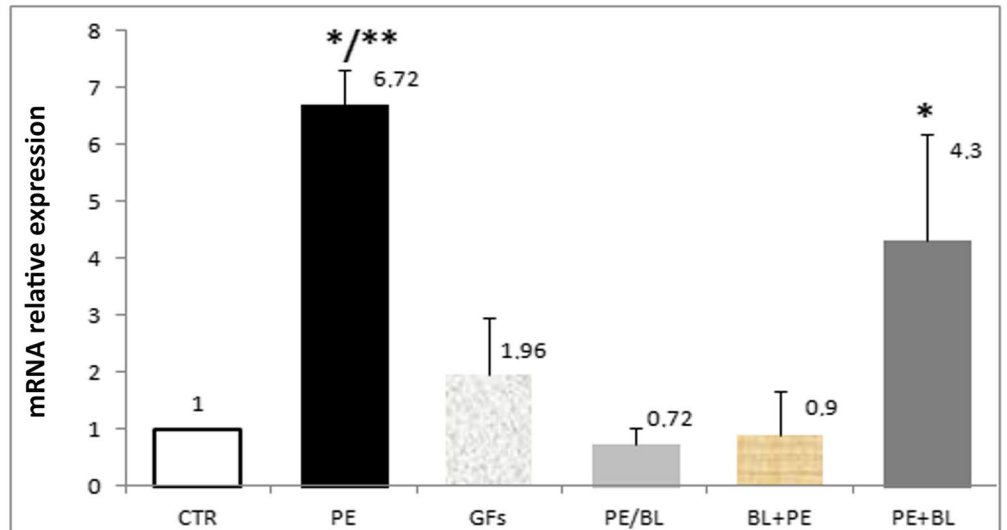
RACK1



MYH7



BNP



endocardium-activated Epicardium expresses NFAT2/GATA4²¹. To determine whether RACK1 is associated with the expression of these embryonal genes, GF-activated cells were transfected with a plasmid containing *rack1/hemagglutinin*-Tag (RACK1/HA) and analysed 24 h after the transfection event (T0, Fig. 6) or for one week (T1, Fig. 7). T1 cells were also cultured in culture media containing GFs to stimulate both the proliferation and expression of embryonic genes. Transfected cells at T0 and T1 were compared to control cells (CTR) that did

◀ **Figure 1.** Quantitative RT-PCR analysis of RACK1 and hypertrophy markers. The graph shows the relative expression of Rack1 (RACK1), myosin heavy chain 7 (MYH7), and brain natriuretic peptide (BNP). In the PE-treated samples, a significant increase in markers was observed compared with those in the control samples (PE vs. CTR; PE vs. all groups $p < 0.001$, *). The GFs group, despite the variability of the samples, was significantly greater than the CTR and the other groups were, except for the PE group (GFs vs. CTR, PE/BL, PE + BL BL + PE, *, $p < 0.01$). The PE/BL and PE + BL groups presented nonsignificant modifications, whereas the BL + PE group presented a reduction (BL + PE vs. CTR, **, $p < 0.05$). MYH7 expression was significantly upregulated in the PE and PE + BL groups (PE vs. CTR, *, PE vs. all groups, **, $p < 0.001$; PE + BL vs. all groups without PE, *, $p < 0.005$). Compared with the CTR group, the GFs group presented a slight increase (GFs vs. CTR, *, $p < 0.05$). BNP was increased in the PE group (PE vs. CTR; $p < 0.001$; *, PE vs. all other groups). **, $p < 0.05$) and the PE + BL group (PE + BL vs. CTR, *, $p < 0.01$). Conversely, this upregulation was partially repressed after pre- and cotreatment with BL. The GFs also presented a greater mean than did the control, but the variability among the samples was not statistically significant. Hearts from the fish in each group ($n = 6$) were subjected to triplicate experiments—statistical analysis: ANOVA with the Bonferroni correction.

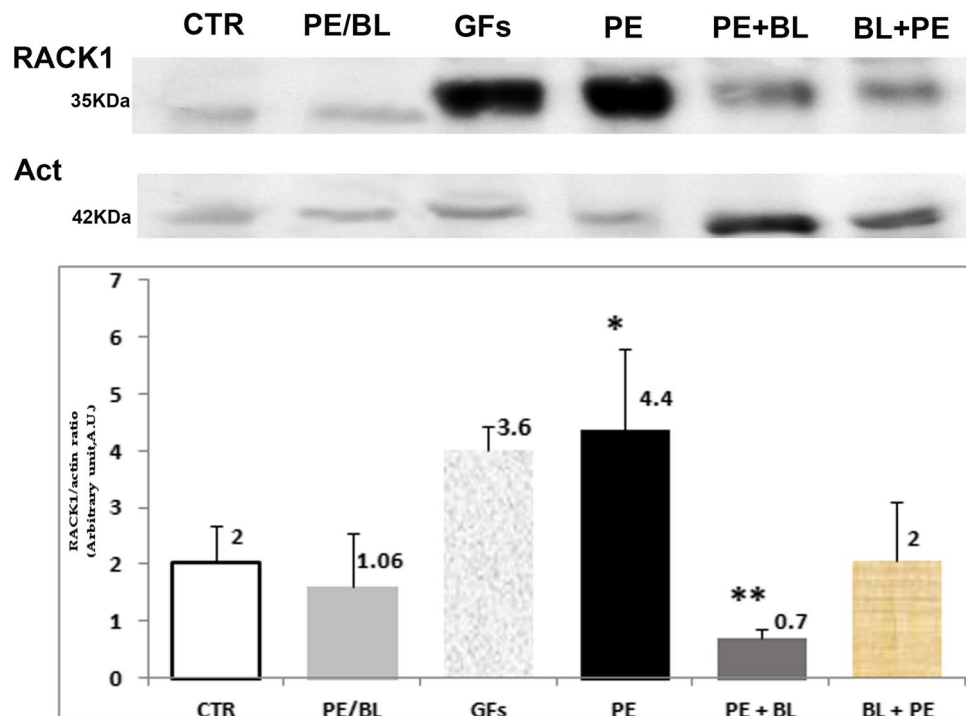


Figure 2. Immunoblot analysis of RACK1 protein expression in the experimental groups vs. CTR. Immunoblot images of Rack1 protein (RACK1) expression (upper part) and nonsarcomere actin (below) were used as housekeeping proteins. The graph shows the means of at least three independent experiments of the density ratio between the RACK1 and actin bands (mean \pm S.D.). Compared with that in the CTR group, RACK1 expression was strongly marked in the PE group ($p < 0.001$, *), but appreciable positivity was also observed in the GFs in the CTR group ($P < 0.05$, *). The level of RACK1 was comparable to that of CTR in the other treatment groups. The PE + BL group expressed less protein than the CTR group did (**; $p < 0.05$). Hearts from the fish used in triplicate experiments ($n = 10$ in each group) were subjected to statistical analysis: ANOVA with the Bonferroni correction.

not contain the plasmid. Immunocytochemistry was conducted with double labelling and an anti-HA antibody to detect RACK1 expression via the plasmid (green fluorescence) and the endogenous embryonic genes GATA4, WT1, and NFAT2 (red fluorescence). The labelling analysis was conducted with a confocal microscope to obtain a clear signal of the labels and evaluate their possible relationship with RACK1 upregulation.

CTR cells did not show any positivity to HA and, therefore, to plasmid-encoded RACK1. These findings also supported the normal expression of endogenous RACK1 at T0 (Fig. 4) and T1 (Fig. 7) due to stimulation by GFs. At T0, the transfected cells all expressed RACK1/HA (Fig. 6), whose presence largely colocalized with GATA4, WT1, and NFAT2 expression.

In particular, GATA4 was more highly expressed in RACK1/HA-positive cells than in CTR cells. Moreover, GATA4 in RACK1/HA cells was locally diffused at the cytoplasmic level but was poorly detectable or comparable to CTR at the nuclear level. At T1, RACK1/HA-positive cells displayed marked expression of GATA4 at both the nuclear and cytoplasmic levels. Figure 7 shows CTR cell labelling at both the nuclear and cytoplasmic levels.

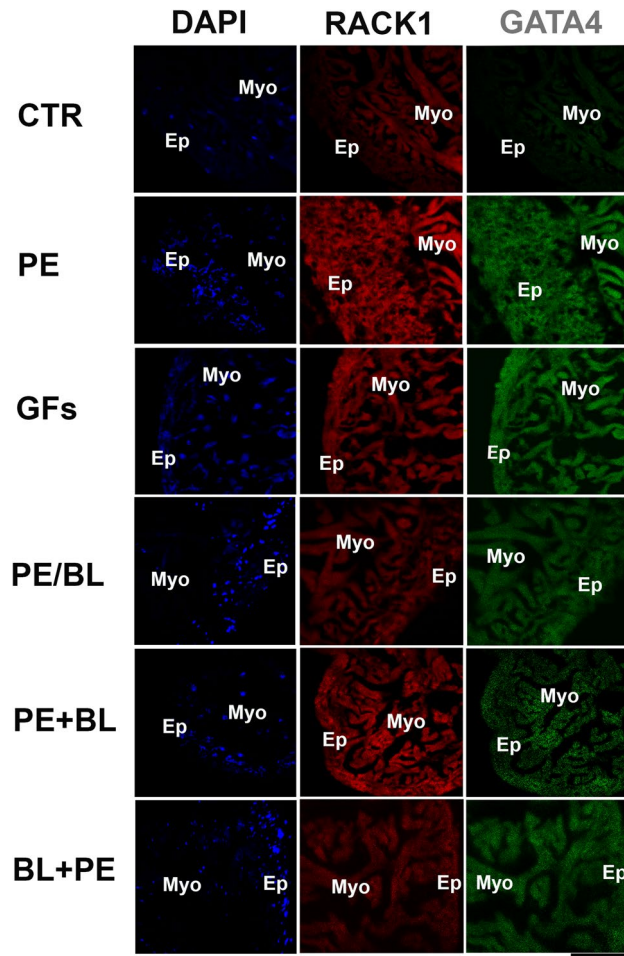


Figure 3. Double staining with RACK1 and GATA4 was analysed via confocal microscopy. RACK1 (red fluorescence) is fundamentally expressed in the CTR myocardium. In all the experimental groups, RACK1 was increased and colocalized with the GATA4 antibody (green fluorescence). GATA4 is strongly expressed in PE and GFs and moderately expressed in PE + BL and PE/BL. Moreover, it was expressed at lower levels in the BL + PE treatment. The hearts utilized for the experiments were $N = 4/5$ sections in each group in triplicate experiments. Blue fluorescence: DAPI (nuclear marker); scale bar: 500 μm .

WT1 expression in the CTR at T0 (Fig. 6) was mild, and WT1 was detected mainly in the nucleus. At T1 (Fig. 7), positivity was detected mainly in the cytoplasm. In RACK1/HA-positive cells, WT1 positivity was mainly nuclear and colocalized in some regions with RACK1/HA positivity.

At T0, NFAT2 (Fig. 6) was positively immunostained, with a few spots at the nuclear level in both RACK1/HA cells and CTRs. At T1 (Fig. 7), the control displayed slightly greater positivity for NFAT2 than at T0, and NFAT2 was also positive at the cytoplasmic level. Interestingly, at T1 in RACK1/HA-transfected cells (Fig. 7), NFAT2 immunostaining became more intense in the cytoplasm than in the nucleus. NFAT2 positivity also appeared to colocalize with RACK1/HA.

Discussion

RACK1 is expressed in cardiac tissue and extensively expressed in PE- and GFs-treated hearts

In ZF, RACK1 has been detected in some organs/tissues, such as the epidermis, intestinal tract, liver²⁴, and cardiovascular system²⁵; however, a possible correlation between RACK1 and embryonal gene expression is rare. Currently, RACK1/embryonal gene correlation is known to be necessary from the gastrula stage to the adult stage because any knockout-RACK1 model is not life compatible²⁶.

In ZF, as well as in mammals, the epithelial cells of the heart undergo proliferation and transdifferentiation by re-expressing embryonal genes when subjected to hypertrophic regeneration²¹. The expression of GATA4, NFAT2, and WT1 embryonal markers appears to be dependent on miR expression¹⁸, possibly involving RACK1 in our previous analysis of their translational control.

In the present research, in the cardiac control group, RACK1 was expressed at low levels and was widespread in the epicardium, myocardium, and endocardium. This observation is consistent with other findings in vertebrate or invertebrate tissues because of the constitutive expression of differentiated cells or a predifferentiating process²⁷. For example, RACK1 is expressed transiently in the skeletal muscle of postnatal mice, is abundant in

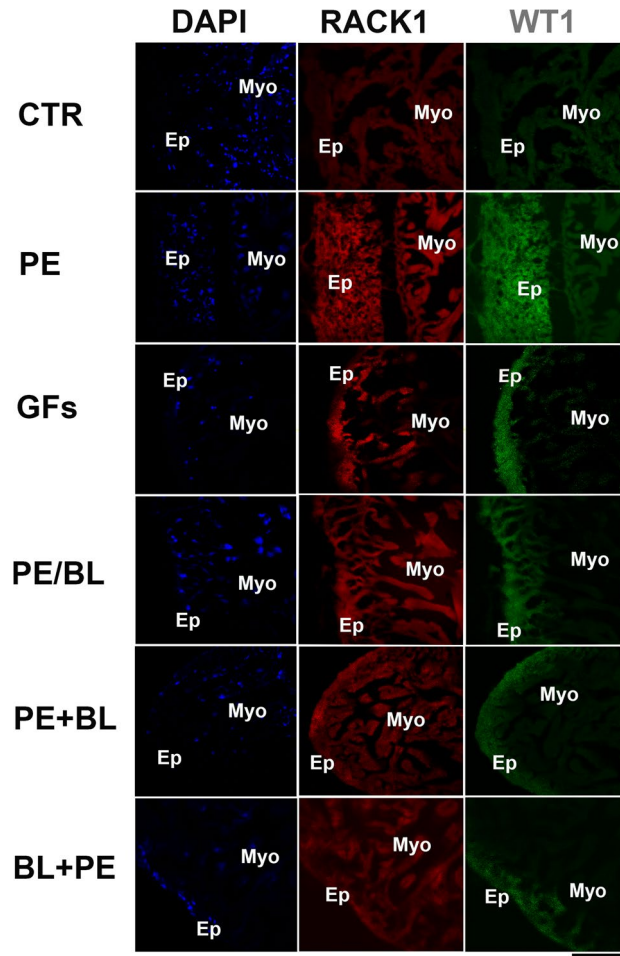


Figure 4. Double staining of RACK1 and WT1 was performed via confocal microscopy. RACK1 (red fluorescence) is expressed at lower levels in the epicardium than in the myocardium in the CTR. In all the experimental groups, RACK1 expression was increased, and RACK1 was particularly colocalized with the WT1 antibody, which stains the epicardium (green fluorescence). WT1 is strongly expressed in PE and GFs and moderately expressed in PE + BL, PE/BL, and BL + PE. The hearts utilized for the experiments were $N=4/5$ sections in each group in triplicate experiments. Blue fluorescence: DAPI (nuclear marker); scale bar: 500 μm .

the early phase of muscle growth and almost disappears in mature adult fibres²⁸. During oogenesis in *Drosophila*, somatic RACK1 plays a non-cell-autonomous role in maintenance and function².

In contrast to that in the CTR- or BL-treated samples, RACK1 expression was markedly increased in the PE-treated samples by approximately sixfold-fold according to qRT-PCR and doubled according to immunoblotting. This observation suggests that RACK1 may be involved in the hypertrophy process. This finding is supported by evidence of high expression of hypertrophy markers, such as MYH7 and BNP, in line with RACK1 expression in different samples. Similarly, heart samples cultured with buffer supplemented with GFs, which has already been standardized in our laboratory²¹, presented a RACK1 expression level that was double that of the CTR.

Previously, in both PEs and GFs, chemostimulation was related to the downregulation of key microRNAs (i.e., miR1, miR133a, and miR133b)^{17,18}. These miRs lead to different pathways that cause cells to differentiate into various cardiac types (epicardial, endocardial, and myocyte) by repressing embryonic gene expression directly or indirectly^{17,18}. In this context, the observation of high expression of RACK1 and, contemporarily, notable embryonic gene expression may indicate direct or indirect relationships between these molecules. Interestingly, the RACK1 mRNA and protein levels in the groups treated with BL were compared. Interestingly, in the pretreatment with BL and in the contemporary treatment with PE and BL, the expression of RACK1 was comparable on average to that in the control. Instead, in the group posttreated with BL (PE + BL), the mRNA level was significantly greater than that in the control, while the protein level appeared to be significantly lower. An explanation could be that, in mammalian cardiomyocytes, the eIF6/p27BBP-his-myc protein complex is also localized in Z discs directly activated by cytoskeletal disruption generated by the BL and is able to decrease protein synthesis by attaching to the 60 S subunit²⁹. Furthermore, eIF6 directly interacts in the cytoplasm, with RACK1 limiting its presence³⁰.

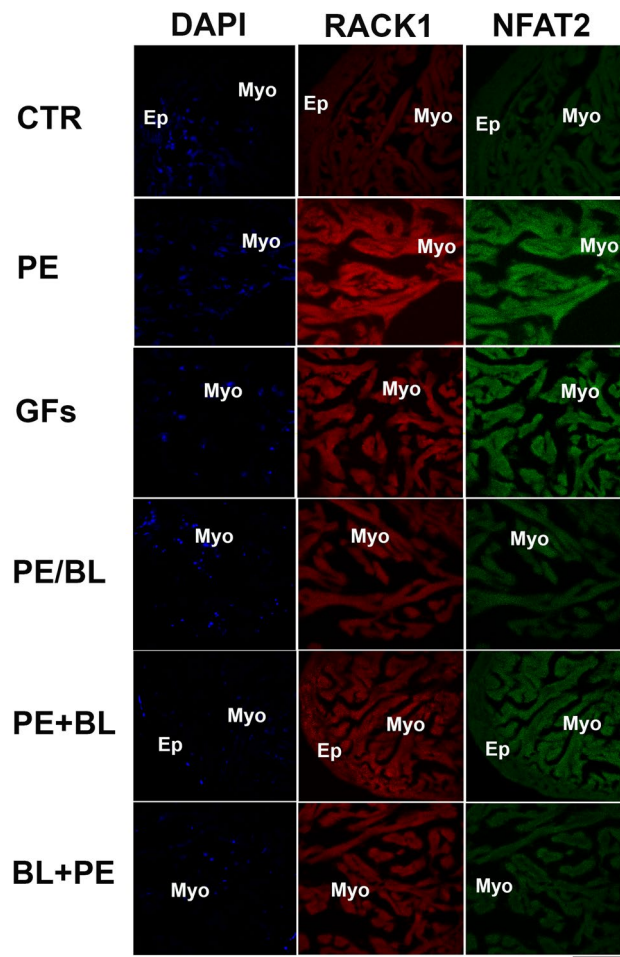


Figure 5. Double staining of RACK1 and NFAT2 was performed via confocal microscopy. RACK1 (red fluorescence) is fundamentally expressed in the myocardium of CTR. In all the experimental groups, RACK1 expression was increased, and RACK1 colocalized with the NFAT2 antibody to mark the endocardium (green fluorescence). NFAT2 is strongly expressed in PE and GFs and moderately expressed in PE + BL, PE/BL, and BL + PE. The hearts utilized for the experiments were $N = 4/5$ sections in each group in triplicate experiments. Blue fluorescence: DAPI (nuclear marker); scale bar: 500 μm .

RACK1 colocalized with embryonal markers in activated cells

The zinc finger protein GATA4 is a hypertrophy-responsive transcription factor in mammals that forms a complex with an intrinsic histone acetyltransferase, p300. Previous studies have indicated that Cdk9 forms a functional complex with p300/GATA4 and is required for the p300/GATA4-transcriptional pathway during cardiomyocyte hypertrophy. RACK1 also plays an important role in this phase^{10,31}. Moreover, in rats, cardiomyocytes cultured with PE block hypertrophy when RACK1 phosphorylation is inhibited¹⁰. In our model of cardiac hypertrophy in the ZF, GATA4 was highly expressed in the PE and GFs groups and was partially expressed in the PE and BL groups compared with the CTR group. These findings, together with high RACK1 expression in PE/samples, contrast with those of Suzuki et al.¹⁰. However, considering the multiple functions of RACK1 in the cytoplasm, we can hypothesize that its major function in PE and GFs is to favour GATA4 translation instead of phosphorylating the p300/GATA4 complex³². Further transfection experiments confirmed this hypothesis (see below).

The Wilms' tumor suppressor gene *wt1* encodes a C protein with four C-terminal Kruppel-type zinc finger transcription factors, which play important roles in the development of the mammalian genitourinary system and heart^{33,34}. The expression of this transcription factor is exclusive to the activated epicardium in mammals as well as in ZF^{18,35}. In ZF, *wt1a*- and *wt1b*-expressing cardiomyocytes exhibited altered cell adhesion properties, delaminated from the myocardium, and upregulated epicardial gene expression, which led to their transdifferentiation into epicardial-like cells³⁶. In the present research, WT1 was highly expressed in the PE- and GF-treated groups compared with the other groups, confirming previous findings. Interestingly, RACK1 colocalized with this gene. WT1⁺ cells show mutually exclusive binding of either protein phosphatase 2 A or integrin to RACK1, which is controlled by an agonist-dependent interaction between RACK1 and the insulin-like growth factor I receptor³⁷. Insulin-dependent regulation of the composition of this RACK1 protein complex impacts cell migration³⁸. Integrins are likely related to hyaluronic acid in the extracellular matrix, which causes

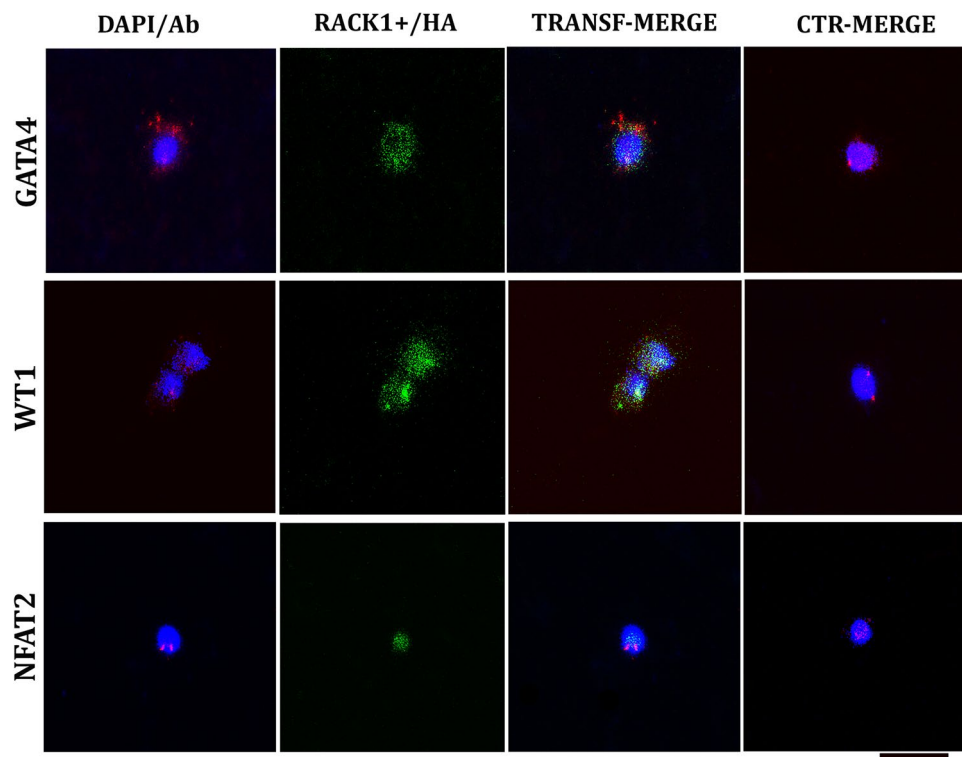


Figure 6. Confocal analysis at 24 h post-transfection (T0). The plasmid containing *rack1*⁺ and the reporter hemagglutinin (RACK1⁺/HA) produced green fluorescence. The cells were double-labelled with embryonal markers (GATA4, WT1, and NFAT2; red fluorescence) and compared to nontransfected cells (CTR). GATA4 is increased in transfected cells and is localized mainly in the cytoplasm. WT1 is comparable to the CTR. NFAT2 is sparsely expressed in the CTR and, in both cases, is localized in the nucleus. The nucleus was labelled with DAPI (blue fluorescence). DAPI/Ab: DAPI-labelled antibody (GATA4, WT1 or NFAT2). TRANSF/MERGE: Transfected cells labelled with all the antibodies (against HA and one embryonal marker). CTR/MERGE: nontransfected cells labelled with all the antibodies. The hearts utilized for the experiments were $N = 4/5$ sections in each group in triplicate experiments. The hearts utilized for the experiments were $N = 3$, and analysis was performed with 10^4 cells in each group in triplicate. Bar: 20 μm .

the cells to migrate after epithelial-mesenchymal transdifferentiation²⁰. In a hypertrophy or regeneration cardiac ex vivo model, WT1 was highly expressed in activated epicardial cells^{18,21}.

NFAT is a family of transcription factors (NFAT 1–5^{39–41}), found in the cytosol in its phosphorylated, inactive form⁴². NFAT2 is mediated by activation and controlled by calcineurin, a Ca^{2+} -dependent phosphatase, and RACK1. At sustained elevations in cytoplasmic calcium, calcineurin dephosphorylates NFATC1–C4, allowing NFAT to translocate to the nucleus and activate gene transcription^{42–44}. NFAT2 is expressed in muscles, including the heart, during differentiation, maturation, and hypertrophy⁴². Transgenic mice with cardiomyocyte-specific G protein-coupled receptor kinase overexpression activate NFAT reporters basally and after hypertrophic stimulation, including transverse aortic constriction and phenylephrine treatment⁴⁴. In ZF, enhanced NFAT2 expression was demonstrated during PE treatment in ex vivo cultured hearts²². In response to PE treatment, calcium waves can activate calmodulin, which, in a cascade, activates serine/threonine phosphatases and calcineurin. The latter can bind to the N-terminal regulatory domain of NFAT, inducing dephosphorylation and conformation changes. In the present study, NFAT2 was enhanced by GF treatment and partially by PE. Interestingly, nickel-enhancement/DAB immunostaining revealed that RACK1 was localized in the endocardium after PE treatment (the PE, PE + BL, PE/BL, and BL + PE groups), demonstrating a role for endocardium activation in hypertrophy. BL and PE treatments, as indicated by their lower expression, align with the previously described Ca^{++} -wave blocking capacity of BL.

Transfection of activated cells with a plasmid containing RACK1/hemagglutinin affected embryonic gene expression

In our ZF model, the activated epicardial and endocardial cells presented RACK1 and basic embryonic gene expression levels of GATA4, WT1, and NFAT2 under L15c without GFs. The myocytes remain in the ex vivo organ; thus, they were used only for histochemical analyses. However, the expression of embryonic genes and RACK1 increased in response to culture with growth factor (GF)-supplemented medium. This observation aligns with our previous observations, indicating enhanced embryonic gene expression²¹. Compared with that in the nontransfected control cells, embryonic gene expression was increased in the activated/RACK1⁺-transfected cells. Moreover, after one week of culture in GFs-supplemented medium, all the genes were strongly expressed

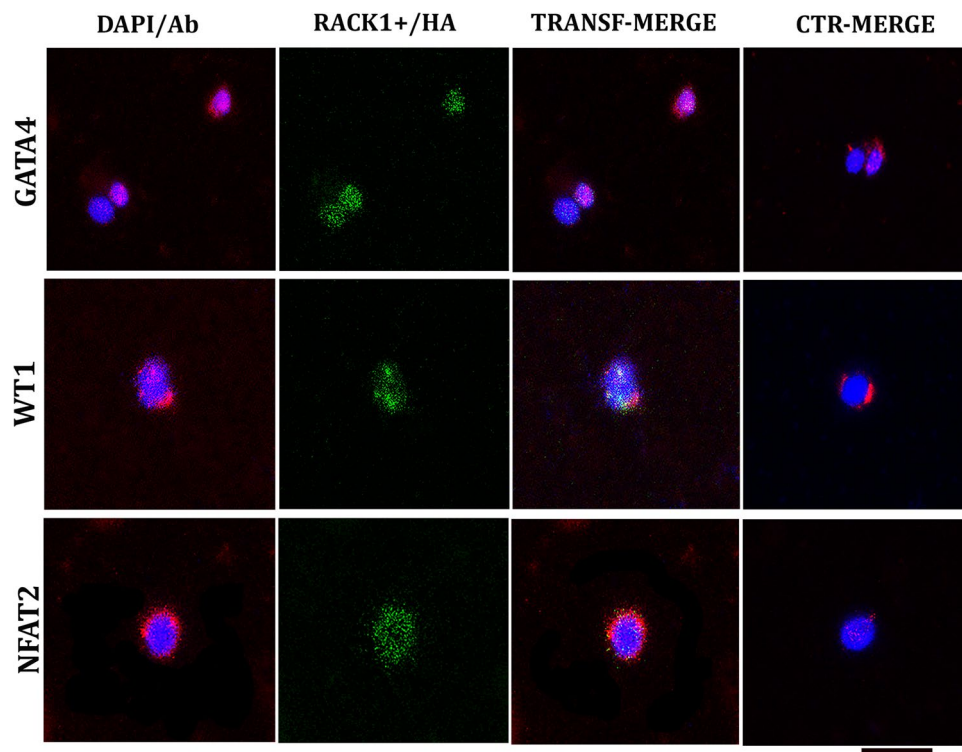


Figure 7. Confocal microscopy analysis after transfection and one week of culture in medium supplemented with GFs (T1). The plasmid containing RACK1/HA emitted green fluorescence. The cells were double-labelled with embryonal markers (GATA4, WT1, and NFAT2; red fluorescence) and compared to nontransfected cells (CTR). GATA4 is strongly increased in transfected cells and is localized mainly in the nucleus. Compared with CTR, WT1 is highly expressed in the nucleus and cytoplasm. Compared with its expression in the nucleus, NFAT2 is more highly expressed in the cytoplasm than CTR, which is localized in the nucleus. Nuclei are marked with DAPI (blue fluorescence); DAPI/Ab: DAPI labelling+ antibody (GATA4 or WT1 or NFAT2). TRANSF/MERGE: transfected cells labelled with all the antibodies (against HA and one embryonal marker). CTR/MERGE: nontransfected cells labelled with all the antibodies. The hearts utilized for the experiments were $N=3$, and analysis was performed with 10^4 cells in each group in triplicate. Bar: 20 μm .

in the transfected cells, suggesting that some RACK1 is involved in their translation. In particular, GATA4 is strongly expressed at the nuclear level in transfected/GFs-cultivated cells. Thus, RACK1 overexpression enhances the presence of the GATA4 protein (detected by specific antibodies) and increases GATA4 activity in the nucleus. Unfortunately, there are no previous reports about the possible role of RACK1 in GATA4 translation.

Epicardium-derived cells, which become activated upon injury and migrate to the injured area, can differentiate into various types of myocardial cells. These cells are WT1 positive in both mammals and fish^{21,45}. WT1, Wilms' tumor suppressor protein, is a zinc finger-containing transcription factor that activates or represses transcription depending on the cell type and promoter context and that adheres to proteins with a WD40 motif⁴⁶. After activation, WT1⁺ cells undergo mesenchymal transition and can activate angiogenesis and a new extracellular matrix by stimulating resident fibroblasts⁴⁷. In this study, WT1 expression was increased in RACK1⁺/HA-transfected cells after 1 week of culture in growth factors (GFs)-supplemented medium and 24 h after transfection. WT1 was localized mainly to the nucleus. Similarly, in nontransfected cells, WT1 expression was also increased after 1 week but was less pronounced than that in the transfected cells. Taken together, these observations suggest a possible role for RACK1 in WT1 protein translation.

NFAT2 is a marker of endocardial-activated cells and is expressed early in ZF development. NFAT can change dynamically in phosphorylation status through the action of additional molecules such as nuclear p300, GATA, and RACK1^{48,49}. After 1 week of culture GFs-supplemented medium, the RACK1⁺/HA cells presented high NFAT2 gene expression. The localization was principally cytoplasmic instead of nuclear. Interestingly, after 1 week of culture in GFs-supplemented medium, NFAT2 expression was significantly greater in RACK1⁺/HA cells than in nontransfected or T0-transfected cells. In previous studies, the overexpression of RACK1 was hypothesized to play a role in NFAT binding and blocking its nuclear translocation⁴⁴. However, in our case, the high presence of NFAT2 in the cytoplasm and nucleus in T1 RACK1/HA-transfected cells could not be explained simply as a block of translocation because it seems to be linked to increased protein translation. Interestingly, when RACK1 expression is decreased by myocardial infarction, cardiomyocytes undergo apoptosis⁴⁹. This observation was confirmed by the blocking of RACK1⁺/HA-transfected cardiomyocyte apoptosis. In this context, the NFAT2 protein may also be involved because it regulates PD-1 (programmed death-1) expression⁵⁰.

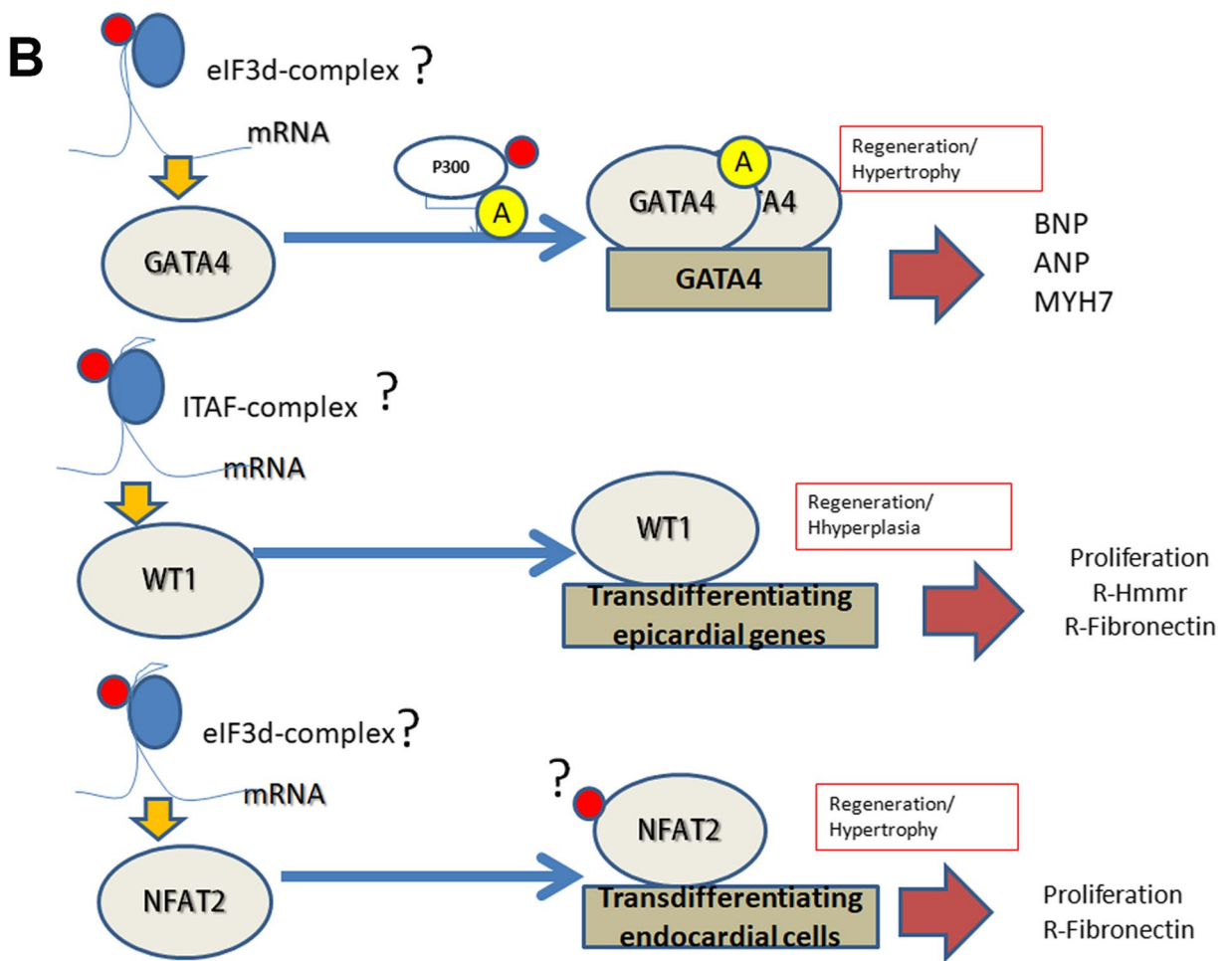
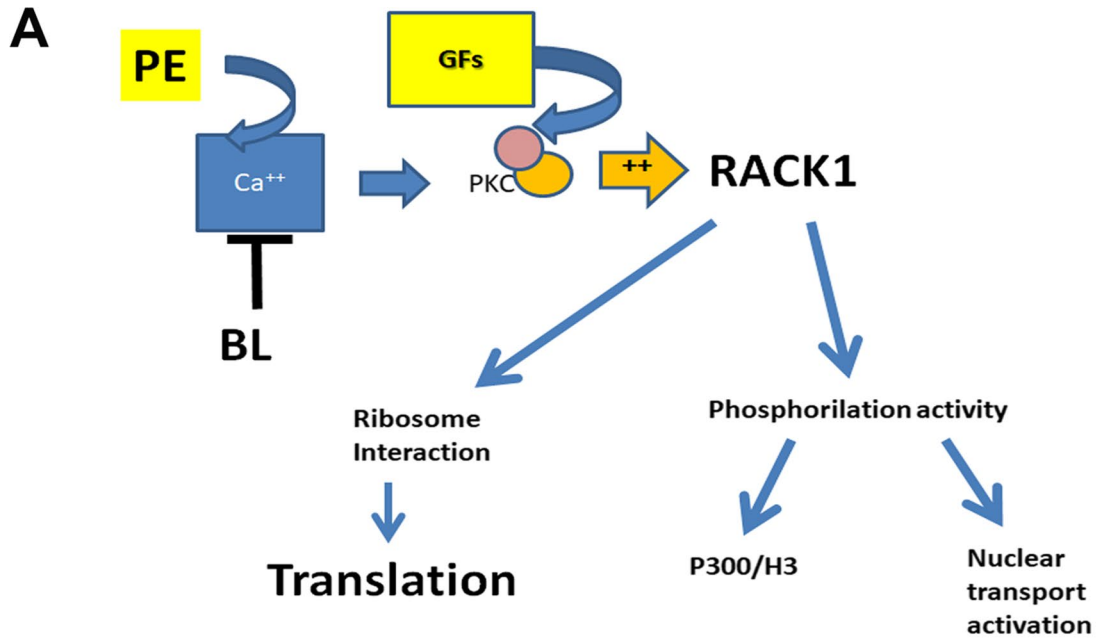
Conclusions and mechanistic hypothesis of RACK1 interactions

RACK1, an adapter protein that interacts with a variety of signalling molecules to promote phosphorylation in combination with PKC^{51–53}, is also a component of the 40S subunit of the ribosome that interacts with Scp160⁵ and is necessary for 60S subunit assembly^{29,54}. In particular, RACK1 may be involved in alternative-translation eIF-3d-dependent processes by attaching to the 5'UTR loop of mRNA^{29,53}. RACK1 is also involved in other alternative translation machinery by functioning as an adapter favouring the ribosome 40S/60S junction in the ITAF-internal ribosome entry site (IRES) complex⁵⁵. The IRES sequence has a longer loop than does the eIF3d dependent, highly structured 5'UTR, which lacks a methylated cap structure at the 5' end and represents the most ancient translation system (conserved from viruses⁴⁰). Since the translated eIF4E-dependent cap represents a recent machinery type in evolution, it is possible that ancient embryonic genes (common in vertebrates) could be translated by the eIF-3d-dependent or IRES-ITAF typology⁴⁰ (Fig. 8).

The present research demonstrated the involvement of RACK1 in heart hypertrophy or GF activation *ex vivo*. In samples treated with PE or GFs, RACK1 was increased, and we observed significant expression of GATA4, WT1, and NFAT2. Several studies in mammals have confirmed that PE stimulation activates signalling pathways associated with cardiomyocyte hypertrophy, including the ERK/JNK/p38 (MAPK), calcineurin-NFAT, JAK/STAT, and p300/GATA4 pathways³². In chickens, fibroblast growth factors induce RACK1, and this induction of RACK1 expression is accompanied by a significant increase in the number of active PKC molecules/PKC enzymatic activity⁵⁶. Thus, it is not surprising that some key embryonic genes are re-expressed by PE in GFs; however, RACK1 may play a role in this process. By overexpressing a plasmid containing *rack1*, we confirmed the involvement of this protein in activating cardiac cells and enhancing embryonic gene expression. Although some remarks can be made regarding the possible outcomes of RACK1 loss of function, this was not investigated in this study. Since loss-of-function or KO models of RACK1 are not viable in mammals^{26,57}, we decided to limit the experiment to overexpression. Further studies on RACK1 should highlight its direct versus indirect involvement in transcribing and translating embryonic genes since an increase in the canonical translation mechanism has also been reported in heart regeneration or hypertrophy⁵⁸. Moreover, RACK1 may be indirectly involved in the translation of specific RBP-bound mRNAs⁵⁹.

Ideally, RACK1 may be involved in eIF-3d-dependent translation and increase the protein level of GATA4 (Fig. 8) or NFAT2. Ongoing bioinformatic analysis revealed a dimensional loop in the 5' mRNA of GATA4 that attaches to the eIF-3d cap complex and thus RACK1, whereas NFAT2 is still difficult to prove. Among the several variants described in WT1 mRNA, there is evidence for a non-AUG (CUG) translation initiation codon upstream of the first AUG. A long 5'UTR sequence, compatible with the IRES sequence, could suggest a possible role of RACK1 in translation [47–51] (Fig. 8). Since NFAT2 translation is increased in transfected cells, RACK1 may also be directly involved in the translation of the protein by interacting with alternative translation machinery. This ancient, early-expressed gene may be derived from alternative translation motifs. Further bioinformatic and experimental tests should be conducted to confirm this hypothesis (Fig. 8).

The signals identified by comparative studies should be the focus of follow-up candidate approaches to determine the exact roles that key signals or genes play in regeneration/disease. They should also investigate how this signal can be manipulated to facilitate reparative process control. In this context, this research highlights RACK1's potential as a candidate marker of cardiac cell activation.



◀ **Figure 8.** RACK1 activation (A) and hypotheses about the possible direct interaction of RACK1 with embryonal marker expression (B). **A**) According to previous studies, RACK1 can be activated by PKC, which, in turn, is activated by calcium waves induced by PE or a cocktail of FGFs (GFs). BL treatment depletes the calcium wave. **B**) The translation of the mRNA of GATA4 could involve the IRES sequence because our bioinformatic analysis revealed a long sequence in the 5' UTR. RACK1 interacts with the ITAF/IRES complex to permit ribosome assembly. The acetylation of GATA4 by the transcriptional coactivator p300 induces its multimerization and activates its DNA binding activity. GATA4 permits the transcription of cardiac hypertrophic response genes, including atrial natriuretic factor (ANF), brain natriuretic peptide (BNP), and myosin heavy chain 7 (MYH7). Preliminary bioinformatic analysis revealed that the long 5'UTR of WT1 is compatible with the IRES sequence. RACK1 can interact with the ITAF/IRES complex for ribosome assembly during translation. WT1, as a transcription factor, can induce epicardial cell proliferation and transdifferentiation. NFAT2 can interact with RACK1 in two ways: translation via the eIF-3d 5'UTR and cooperation in transporting the phosphorylated protein to the nucleus. NFAT2 is a powerful transcription factor for the proliferation and transdifferentiation of the endocardium and endothelial cells.

Data availability

STATEMENT OF DATA AVAILABILITY. All authors have seen and approved the submitted manuscript's final version. All data generated or analysed during this study are included in this published article and in its supplementary files. Further data can be available from the corresponding author on reasonable request.

Received: 30 July 2024; Accepted: 10 October 2024

Published online: 28 October 2024

References

- Buoso, E. et al. Transcriptional regulation of RACK1 and modulation of its expression: role of steroid hormones and significance in health and aging. *Cell. Signal.* **35**, 264–271. <https://doi.org/10.1016/j.cellsig.2017.02.010> (2017).
- Kadrmaz, J. L., Smith, M. A., Pronovost, S. M. & Beckerle, M. C. Characterization of RACK1 function in Drosophila development. *Dev. Dyn.* **236**, 2207–15. <https://doi.org/10.1002/dvdy.21217> (2007) (PMID: 17584887).
- Adams, D. R., Ron, D. & Kiely, P. A. RACK1, a multifaceted scaffolding protein: structure and function. *Cell. Commun. Signal.* **9**, 22. <https://doi.org/10.1186/1478-811X-9-22> (2011).
- Bass-Stringer, S., Tai, C. M. K. & McMullen, J. R. IGF1-PI3K-induced physiological cardiac hypertrophy: implications for new heart failure therapies, biomarkers, and predicting cardiotoxicity. *J. Sport Health Sci.* **10**(6), 637–647 (2021). Epub 2020 Nov 24. PMID: 33246162; PMCID: PMC8724616.
- Nilsson, J., Sengupta, J., Frank, J. & Nissen, P. Regulation of eukaryotic translation by the RACK1 protein: a platform for signalling molecules on the ribosome. *EMBO*. **5**, 1137–1141 (2004).
- Ceci, M., Fazi, F. & Romano, N. The role of RNA-binding and ribosomal proteins as specific RNA translation regulators in cellular differentiation and carcinogenesis. *BBA Mol. Basis Dis.* **1867**(4), 166046. <https://doi.org/10.1016/j.bbadis.2020.166046> (2021). Epub 2020 Dec 28. PMID: 33383105.
- Romano, N. et al. Ribosomal RACK1 regulates the dendritic arborization by repressing FMRP activity. *Int. J. Mol. Sci.* **23**, 11857. <https://doi.org/10.3390/ijms231911857> (2022).
- Iwasaki, S., Kawamata, T. & Tomari, Y. Drosophila argonaute1 and argonaute2 employ distinct mechanisms for translational repression. *Mol. Cell.* **34**, 58–67. <https://doi.org/10.1016/j.molcel.2009.02.010> (2009).
- Jannot, G. et al. The ribosomal protein RACK1 is required for microRNA function in both *C. Elegans* and humans. *EMBO Rep.* **12**, 581–586. <https://doi.org/10.1038/embor.2011.66> (2011). Epub 2011 Apr 28. PMID: 21525958; PMCID: PMC3128278.
- Suzuki, H. et al. Tyrosine phosphorylation of RACK1 triggers cardiomyocyte hypertrophy by regulating the interaction between p300 and GATA4. *Biochim. Biophys. Acta.* **1862**(9), 1544–1557. <https://doi.org/10.1016/j.bbadis.2016.05.006> (2016).
- Volta, V. et al. RACK1 depletion in a mouse model causes lethality, pigmentation deficits and reduction in protein synthesis efficiency. *Cell. Mol. Life Sci.* **70**(8), 1439–1450 (2013).
- Pass, J. M. et al. Enhanced PKC beta II translocation and PKC beta II-RACK1 interactions in PKC epsilon-induced heart failure: a role for RACK1. *Am. J. Physiol. Heart Circ. Physiol.* **281**, H2500–H2510. <https://doi.org/10.1152/ajpheart.2001.281.6.H2500> (2001).
- Kong, P., Christia, P. & Frangogiannis, N. G. The pathogenesis of cardiac fibrosis. *Cell. Mol. Life Sci.* **71**, 549–574. <https://doi.org/10.1007/s00018-013-1349-6> (2014).
- Frangogiannis, N. G. Cardiac fibrosis: cell biological mechanisms, molecular pathways and therapeutic opportunities. *Mol. Aspects Med.* **65**, 70–99. <https://doi.org/10.1016/j.mam.2018.07.001> (2019).
- Carè, A. et al. MicroRNA-133 controls cardiac hypertrophy. *Nat. Med.* **13**, 613–618. <https://doi.org/10.1038/nm1582> (2007).
- Yang, W. et al. Substrate-dependent interaction of SPOP and RACK1 aggravates cardiac fibrosis following myocardial infarction. *Cell. Chem. Biol.* **30**(10), 1248–1260e4. <https://doi.org/10.1016/j.chembiol.2023.06.015> (2023).
- Romano, N. & Ceci, M. Are microRNAs responsible for cardiac hypertrophy in fish and mammals? What we can learn in the activation process in a zebrafish ex-vivo model. *BBA Mol. Basis Dis.* **1866**, 11–20. <https://doi.org/10.1016/j.bbadis.2020.165896> (2020). Article n. 165896.
- Ceci, M. et al. Micro RNAs are involved in activation of epicardium during zebrafish heart regeneration. *Cell. Death Discov.* **4**, 41. <https://doi.org/10.1038/s41420-018-0041-x> (2018).
- Hu, B. et al. Origin and function of activated fibroblast states during zebrafish heart regeneration. *Nat. Genet.* **54**, 1227–1237. <https://doi.org/10.1038/s41588-022-01129-5> (2022).
- Herada, M. et al. MicroRNA regulation and cardiac calcium signaling role in cardiac disease and therapeutic potential. *Circ. Res.* **114**, 689–705. <https://doi.org/10.1161/CIRCRESAHA.114> (2014).
- Romano, N. & Ceci, M. The face of epicardial and endocardial derived cells in zebrafish. *Exp. Cell. Res.* **369**, 166–175. <https://doi.org/10.1038/s41419-018-0609-7> (2018).
- Bonvissuto, D. et al. Can Blebbistatin block the hypertrophy status in the zebrafish ex-vivo cardiac model? *BBA - Mol. Basis Dis.* **1868**(166471), 0925–4439. <https://doi.org/10.1016/j.bbadis.2022.166471> (2022).
- Dalby, B. et al. Advanced transfection with lipofectamine 2000 reagent: primary neurons, siRNA, and high-throughput applications. *Methods.* **33**(2), 95–103. <https://doi.org/10.1016/j.ymeth.2003.11.023> (2004).
- Kowalewski, J. et al. Characterization of a member of the CEACAM protein family as a novel marker of proton pump-rich ionocytes on the zebrafish epidermis. *PLoS One.* **16**, e0254533 (2021).

25. Kalén, M. et al. Hellström M. Combination of reverse and chemical genetic screens reveals angiogenesis inhibitors and targets. *Chem. Biol.* **16**, 432–441 (2009).
26. Gallo, S. et al. RACK1 specifically regulates translation through its binding to ribosomes. *Mol Cell Biol.* **38**, e00230-18. <https://doi.org/10.1128/MCB.00230-18> (2018) (Erratum in: *Mol Cell Biol.* 2019 Jan 16;39(3): PMID: 30201806; PMCID: PMC6234289).
27. Li, S. et al. RACK1 is required for Vangl2 membrane localization and planar cell polarity signaling while attenuating canonical Wnt activity. *PNAS* **108**, 2264–2269 (2011).
28. Catalani, E. et al. Cervia D. RACK1 is evolutionary conserved in satellite stem cell activation and adult skeletal muscle regeneration. *Cell. Death Discov.* **8**, 459. <https://doi.org/10.1038/s41420-022-01250-8> (2022).
29. Romano, N., Ricciardi, S., Gallo, P. & Ceci, M. Upregulation of eIF6 inhibits cardiac hypertrophy induced by phenylephrine. *Biochem. Biophys. Res. Commun.* **495**, 601–606. <https://doi.org/10.1016/j.bbrc.2017.11.046> (2018).
30. Ceci, M. et al. Release of eIF6 (p27BBP) from the 60S subunit allows 80S ribosome assembly. *Nature.* **426**, 579–584 (2003).
31. Sunagawa, Y. et al. Cyclin-dependent kinase-9 is a component of the p300/GATA4 complex required for phenylephrine-induced hypertrophy in cardiomyocytes. *J. Biol. Chem.* **285**(13), 9556–9568. <https://doi.org/10.1074/jbc.M109.070458> (2010).
32. Shimizu, S. et al. Multimerization of the GATA4 transcription factor regulates transcriptional activity and cardiomyocyte hypertrophic response. *Int. J. Biol. Sci.* **18**, 1079–1095. <https://doi.org/10.7150/ijbs.65664> (2022). PMID: 35173540; PMCID: PMC8771830.
33. Kent, J., Coriat, A. M., Sharpe, P. T., Hastie, N. D. & van Heyningen, V. The evolution of WT1 sequence and expression pattern in the vertebrates. *Oncogene* **11**, 1781–92 (1995) (PMID: 7478606).
34. Bollig, F. et al. Identification and comparative expression analysis of a second wt1 gene in zebrafish. *Dev. Dyn.* **235**(2), 554–61. <https://doi.org/10.1002/dvdy.20645> (2006) (PMID: 16292775).
35. van Wijk, B., Gunst, Q. D., Moorman, A. F. & van den Hoff, M. J. Cardiac regeneration from activated epicardium. *PLoS One.* **7**(9), e44692. <https://doi.org/10.1371/journal.pone.0044692> (2012). Epub 2012 Sep 20. PMID: 23028582; PMCID: PMC3447884e44692.
36. Marques, I. J. et al. Mercader N. Wt1 transcription factor impairs cardiomyocyte specification and drives a phenotypic switch from myocardium to epicardium. *Development.* **149**, dev200375. <https://doi.org/10.1242/dev.200375> (2022).
37. Kiely, P. A., Sant, A. & O'Connor, R. RACK1 is an insulin-like growth factor 1 (IGF-1) receptor-interacting protein that can regulate IGF-1-mediated akt activation and protection from cell death. *J. Biol. Chem.* **277**, 22581–22589. <https://doi.org/10.1074/jbc.M201758200> (2002). Epub 2002 Apr 18. PMID: 11964397.
38. Kiely, P. A., O'Gorman, D., Luong, K., Ron, D. & O'Connor, R. Insulin-like growth factor I controls a mutually exclusive association of RACK1 with protein phosphatase 2A and beta1 integrin to promote cell migration. *Mol. Cell. Biol.* **26**, 4041–4051 (2006).
39. Rao, A., Luo, C. & Hogan, P. G. Transcription factors of the NFAT family: regulation and function. *Annu. Rev. Immunol.* **15**, 707–747. <https://doi.org/10.1146/annurev.immunol.15.1.707> (1997).
40. Rao, A. et al. The translation initiation factor homolog eif4e1c regulates cardiomyocyte metabolism and proliferation during heart regeneration. *Development.* **150**(20), 201376. <https://doi.org/10.1242/dev.201376> (2023).
41. Kar, P. & Parekh, A. B. Distinct spatial Ca²⁺ signatures selectively activate different NFAT transcription factor isoforms. *Mol. Cell.* **58**, 232–243. <https://doi.org/10.1016/j.molcel.2015.02.027> (2015). Epub 2015 Mar 26. PMID: 25818645; PMCID: PMC4405353.
42. Kudryavtseva, O., Aalkjær, C. & Matchkov, V. V. Vascular smooth muscle cell phenotype is defined by Ca²⁺-dependent transcription factors. *FEBS J.* **280**, 5488–5499. <https://doi.org/10.1111/febs.12414> (2013).
43. Han, J. et al. RACK-1, a receptor for activated C kinase, interacts with the transcription factor NFAT and represses its transactivation. *Mol. Cells.* **14**(3), 420–424 (2002). PMID: 12521306.
44. Hullmann, J. E. et al. J. GRK5-mediated exacerbation of pathological cardiac hypertrophy involves facilitation of nuclear NFAT activity. *Circ. Res.* **115**(12), 976–985. <https://doi.org/10.1161/CIRCRESAHA.116.304475> (2014).
45. Gittenberger-de Groot, A. C., Winter, E. M. & Poelmann, R. E. Epi cardium-derived cells (EPDCs) in development, cardiac disease and repair of ischemia. *J. Cell. Mol. Med.* **14**(5), 1056–1060 (2010).
46. Johnstone, R. W. et al. Cio 1 is a novel WD40 protein that interacts with the tumor suppressor protein WT1. *J. Biol. Chem.* **273**, 10880–7. <https://doi.org/10.1074/jbc.273.18.10880> (1998) (PMID: 9556563).
47. Saifi, O., Ghandour, B., Jaalouk, D., Refaat, M. & Mahfouz, R. Myocardial regeneration: role of epicardium and implicated genes. *Mol. Biol. Rep.* **46**, 6661–6674. <https://doi.org/10.1007/s11033-019-05075-0> (2019).
48. Gurung, S., Restrepo, N. K., Chestnut, B. & Klimkaite, S. Single-cell transcriptomic analysis of vascular endothelial cells in zebrafish embryos. *Sci. Rep.* **12**, 13065. <https://doi.org/10.1038/s41598-022-17127-w> (2022).
49. Qian, L. et al. Downregulation of RACK1 is associated with cardiomyocyte apoptosis after myocardial ischemia/reperfusion injury in adult rats. *Vitro Cell. Dev. Biol. Anim.* **52**(3), 305–313. <https://doi.org/10.1007/s11626-015-9981-0> (2016).
50. Oestreich, K. J., Yoon, H., Ahmed, R. & Boss, J. M. NFATc1 regulates PD-1 expression upon T cell activation. *J. Immunol.* **181**, 4832–4839. <https://doi.org/10.4049/jimmunol.181.7.4832> (2008).
51. Johnson, A. G. et al. RACK1 on and off the ribosome. *RNA.* **25**, 881–895. <https://doi.org/10.1261/rna.071217.119> (2019).
52. Coyle, S. M., Gilbert, W. V. & Doudna, J. A. Direct link between RACK1 function and localization at the ribosome in vivo. *Mol. Cell. Biol.* **29**, 1626–1634. <https://doi.org/10.1128/MCB.01718-08> (2009).
53. Rollins, M. G. et al. Negative charge in the RACK1 loop broadens the translational capacity of the human ribosome. *Cell. Report.* **36**, 109663. <https://doi.org/10.1016/j.celrep.2021.109663> (2021). ISSN 2211–1247..
54. Silvestri, F. et al. The ribosomal scaffolding RACK1 is critically required for eIF3d binding to 43S PIC to regulate the HSP-70 protein synthesis. submitted. (2024).
55. Majzoub, K. et al. RACK1 controls IRES-mediated translation of viruses. *Cell.* **159**, 1086–1095. <https://doi.org/10.1016/j.cell.2014.10.041> (2014).
56. Lu, H. C., Swindell, E. C., Sierralta, W. D., Eichele, G. & Thaller, C. Evidence for a role of protein kinase C in FGF signal transduction in the developing chick limb bud. *Development.* **128**(13), 2451–2460. <https://doi.org/10.1242/dev.128.13.2451> (2001).
57. Grosso, S., Volta, V., Sala, L. A., Marchisio, P. C. & Ron, D. Biffo S. PKCβII modulates translation independently from mTOR and through RACK1. *Biochem. J.* **415**, 77–83. <https://doi.org/10.1042/BJ20080463> (2008).
58. Park, S., Nguyen, N. B., Pezhouman, A. & Ardehali, A. Cardiac fibrosis: potential therapeutic targets. *Trans. Res.* **209**, 121–137 (2019).
59. Cheng, F., Pai, R. K. & Cartwright, C. A. Rack1 function in intestinal epithelia: Regulating crypt cell proliferation and regeneration and promoting differentiation and apoptosis. *Am. J. Physiol.-Gastrointestinal Liver Physiol.* **318**, G1–G13 (2018) <https://doi.org/GI-00240-2017>.

Acknowledgements

Acknowledgments: The authors are indebted to Dr. Silvia Bongiorni for the help in bioinformatics analysis of Gata4, Wt1 and Nfat2 zebrafish sequences and to Prof. Francesco Fazi and Dr. Riccardo Marangon for some help in immunocytochemical experiments.

Disclosures

The authors declare that they have no conflicts of interest. The authors did not use generative AI or AI-assisted technologies in the development of this manuscript.

Author contributions

Author Contributions: Conceptualization, N.R.; methodology, M.C., C.S., D.B.; software, E.C.; validation, F.P., F.S.; formal analysis, D.B., F.P and E.C.; investigation, N.R.; resources, D.C. and R.G.; data curation, D.B. and F.S.; writing—original draft preparation, N.R.; writing—review and editing, N.R, M.C.; visualization, R.G and C.S.; supervision, NR. and C.S.; funding acquisition, D.C. All authors have read and agreed to the published version of the manuscript.”

Funding

This research was funded by the Ministry for Universities and Research (MUR): PRIN n.2017FJSM9S_003; Programma Nazionale di Ricerche in Antartide (PNRA) n. PNRA 0000022.

Declarations

Competing interests

The authors declare no competing interests.

Additional information

Supplementary Information The online version contains supplementary material available at <https://doi.org/10.1038/s41598-024-76138-x>.

Correspondence and requests for materials should be addressed to N.R.

Reprints and permissions information is available at www.nature.com/reprints.

Publisher's note Springer Nature remains neutral with regard to jurisdictional claims in published maps and institutional affiliations.

Open Access This article is licensed under a Creative Commons Attribution-NonCommercial-NoDerivatives 4.0 International License, which permits any non-commercial use, sharing, distribution and reproduction in any medium or format, as long as you give appropriate credit to the original author(s) and the source, provide a link to the Creative Commons licence, and indicate if you modified the licensed material. You do not have permission under this licence to share adapted material derived from this article or parts of it. The images or other third party material in this article are included in the article's Creative Commons licence, unless indicated otherwise in a credit line to the material. If material is not included in the article's Creative Commons licence and your intended use is not permitted by statutory regulation or exceeds the permitted use, you will need to obtain permission directly from the copyright holder. To view a copy of this licence, visit <http://creativecommons.org/licenses/by-nc-nd/4.0/>.

© The Author(s) 2024